Time and strain-rate effects on the stress-strain behaviour of soft Hong Kong marine deposits

Effets de temps et de contrainte-cadence sur le comportement de contrainte-tension des dépôts mous de marine de Hong Kong

Jian-Hua Yin – *Department of Civil & Structural Engineering, The Hong Kong Polytechnic University, Hong Kong, China*

ABSTRACT: Hong Kong marine deposits (HKMD) are considered to be difficult soils for civil projects due to low shear strength and time-dependent high compressibility. Understanding the time-dependent stress-strain behaviour of HKMD is of practical significance. In this paper, test data on the time-dependent behaviour of a remoulded HKMD are presented, analysed and discussed.

RESUME: Les dépôts marins de Hong Kong (HKMD) sont considérés les sols difficiles pour des projets civils dus à la basse résistance au cisaillement et à la compressibilité élevée dépendant du temps. La compréhension du comportement dépendant du temps de contrainte-tension de HKMD est d'importance pratique. En cet article, les essais sur le comportement dépendant du temps de a remoulded HKMD sont présentés, analysés et discutés.

1 INTRODUCTION

Massive reclamation on marine deposits in Hong Kong's coastal waters has been constructed in the past decades. More reclamation is to be built in the foreseeable future. The Hong Kong marine deposits (HKMD) are normally greenish grey silty clay or clayey silt and sand with shell fragments. The thickness of HKMD may vary from a few meters to more than 30 meters. HKMD are considered to be difficult (or weak) soils due to low shear strength and time-dependent high compressibility. The stress-strain behaviour of HKMD is non-linear, irreversible and time-dependent. The design of reclamation and structures directly and indirectly on or in the HKMD needs a good understanding of the time-dependent stress-strain behaviour of the HKMD.

In this paper, the time-dependent stress-strain behaviour of HKMD is investigated by oedometer tests and four types of triaxial tests. The data are analysed and discussed with a special interest in the time-dependency, such as, creep, strain rate effects, relaxation, *etc.*, of the stress-strain behaviour of the HKMD and its constitutive modelling.

2 TEST PROGRAM AND BASIC SOIL PROPERTIES

The soil used in the test study is soft Hong Kong Marine Deposits (HKMD) taken from a coastal area near Tai Kowk Tsui harbour in Hong Kong. The HKMD consisted of clay, silts with some fine sand (27.5% clay with particle size <0.002mm, 46.5% silt with 0.002mm< particle size < 0.063mm and 26.0% fine sand with 0.063mm < particle size < 0.15mm). The shell fragments in the natural HKMD were removed in order to have uniform soils for consistent comparative testing study. Therefore, the HKMD samples used in all tests were remoulded soil. The HKMD samples were re-consolidated in a cylindrical stainless steel container that is 30cm in diameter and 60 cm in height under a pressure of about 30 kPa. This re-consolidation was a simulation of the HKMD, for example, under the sand fill loading in reclamation projects and also made the HKMD stiff enough to be trimmed into triaxial specimens. A specimen was prepared by pushing a PVC tube (thin wall) into the re-consolidated HKMD in the cylindrical stainless steel container. The specimen formed by the PVC tube was 50 mm in diameter and 100mm in height.

Basic physical properties of the HKMD were measured. It was found that specific gravity $G_s = 2.66$, liquid limit $w_l = 60\%$, plastic limit $w_p = 28\%$, plastic index $I_p = 32\%$, and water content after re-consolidation $w = 51.7\%$. Both oedometer and triaxial tests were conducted. Conventional triaxial compression shear tests were performed on a Wykeham Farrance triaxial testing machine. Special tests (*e.g.* extension shear and constant-q-rate shear) and some conventional compression shear tests were carried out using a computerised GDS triaxial testing system with stress-path control. In all tests, a back pressure of 200 kPa was applied. The B-value was checked and found to be 0.98 to ensure saturation.

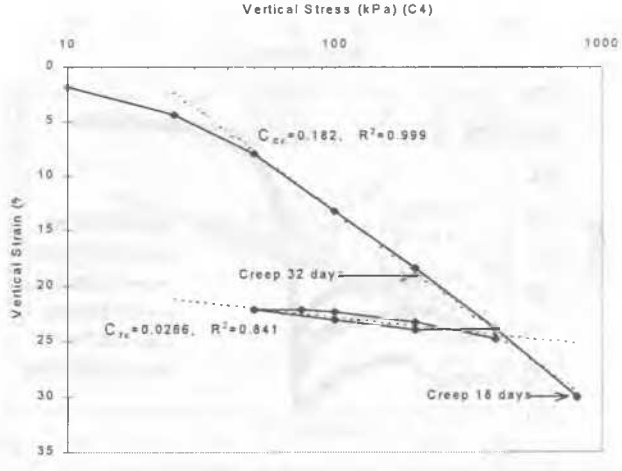

Figure 1. Vertical strain *vs.* log(stress) with loading, unloading and reloading for HKMD

3 MAIN OEDOMETER TEST RESULTS

Main oedometer test results of vertical strain *vs.* log(time) for the HKMD (C4) are obtained. Measured data and best-fitting lines of the vertical strain *vs.* log(stress) are presented in Fig.1.

The compression index C_c, unloading/reloading (or swelling) index C_r, the coefficient of "secondary" consolidation $C_{\alpha\varepsilon}$ and the coefficient of consolidation C_v have been determined using

the test data. Additional tests have been conducted for HKMD with different clay contents. From all these results, the following correlations are obtained

$$C_c = 0.0138 I_p + 0.00732 \quad (1)$$

$$C_r = 0.00219 I_p - 0.0104 \quad (2)$$

$$C_{\alpha\varepsilon} = 0.000369 I_p - 0.00055 \quad (3)$$

where the plasticity index I_p in percentage (%) is in percentage. The correlations in Eqn.(1), (2) and (3) are very close to the correlations reported by Nakase *et al.* (1988) for both Kawasaki clay (mixture series) and reconstituted natural marine clay.

4 TRIAXIAL TEST RESULTS AND DISCUSSION

4.1 *Strain rate effects*

To examine strain rate effects of HKMD under triaxial compression and extension states, three different strain rates were used, *i.e.* 0.25%/min, 0.025%/min and 0.0025%/min and the effective consolidation pressure was 400 kPa. Fig.2(a) shows the relationship of axial strain ε_a *versus* deviator stress q. The smaller the strain rate, the lower the peak shear strength and the higher the porewater pressure generated before failure as shown in Fig.2(a) and Fig.2(b).

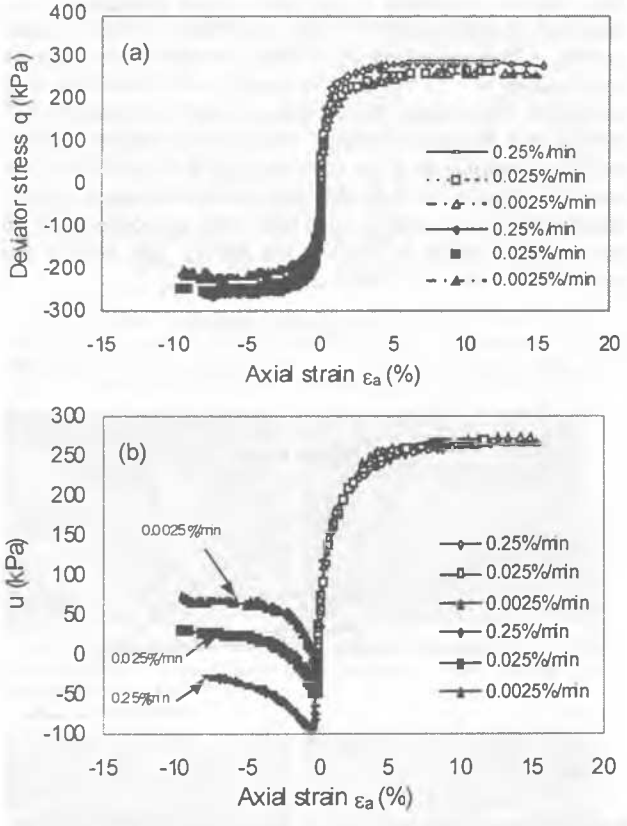

Fig.2(a) Axial strain *vs.* deviator stress and (b) axial strain *vs.* porewater pressure in compression and extension at different strain rates

The change in undrained shear strength with strain rate can be generally described by the parameter ρ_{01}. The parameter ρ_{01} is defined as the change in shear strength caused by a tenfold change in strain rate, expressed as a percentage of the shear strength measured at strain rate 0.1% per hour (Graham *et al.* 1983). For convenience, ρ_{015} was used here because the lowest strain rate in conventional shear tests is 0.0025%/min, that is, 0.15%/h, and no test at a strain rate of 0.1%/h was conducted in our study. From Table 1, we find that the average value of ρ_{015} is 4.9% for compression tests and 9.3% for extension tests. The ε_{af} corresponding to peak deviator stress q_f for the compression tests is larger than that for extension tests.

As shown in Fig.2(b) and Table 1, the excess porewater pressure at failure increases with the decrease of strain rate both under compression and extension tests. However, the response of porewater pressure in specimens under compression states is quite different from that of specimens under extension states. Firstly, the strain rate effects on the excess porewater pressure of the specimen in an extension state are more significant than the effects in a compression state. The ratio of the porewater pressure at failure to effective confining pressure (u_f/σ_h') changes only about 0.01 per logarithm cycle of strain rate in compression tests, but about 0.12 in extension tests. Secondly, the curves of porewater pressure *v.s.* axial strain in extension show clearly a peak, which is different from those curves in compression. This difference is mainly due to that in extension the lateral stress σ_h is the major principle stress, that is, $\sigma_h = \sigma_1$, and the vertical stress is the minor principle stress, that is, $\sigma_v = \sigma_3$. This results in that the total stress path in extension is different from that in compression and the porewater pressure responses are different.

Table 1. Results of conventional undrained triaxial tests under different strain rate $\dot{\varepsilon}_a$

Type of Tests	$\dot{\varepsilon}_a$ (%/min)	q_f (kPa)	ε_{af} (%)	u_f/σ_h'
Compression	0.25	290.0	9.1	0.650
	0.025	268.1	11.5	0.677
	0.0025	264.1	10.6	0.681
Extension	0.25	-258.4	7.3	-0.067
	0.025	-246.3	7.7	0.071
	0.0025	-218.0	7.1	0.168

Notes: σ_h' = effective confining pressure; ε_{af} = axial strain at failure in absolute value; u_f = excess porewater pressure at failure; q_f = deviator stress at peak (failure).

Figs.3(a) and 3(b) show the relationship of the normalized shear strength (q_f/σ_h') and excess porewater pressure (u_f/σ_h') at failure versus axial strain rate (log scale). The relationship between q_f/σ_h' (or u_f/σ_h') and the log(strain rate) appears to be linear for the range of strain rates in the tests.

4.2 *Results of Stress Relaxation Tests*

In a single-stage relaxation tests, a specimen was sheared at a constant strain rate to a given level of strain, which was held constant while the continuously decreasing deviator stress was observed. The results of single-stage stress relaxation tests of six specimens are presented in this section. All specimens were firstly sheared to failure at a strain rate ranging from 0.001%/min

to 0.41%/min under undrained compression or extension states. Then stress relaxation tests were started.

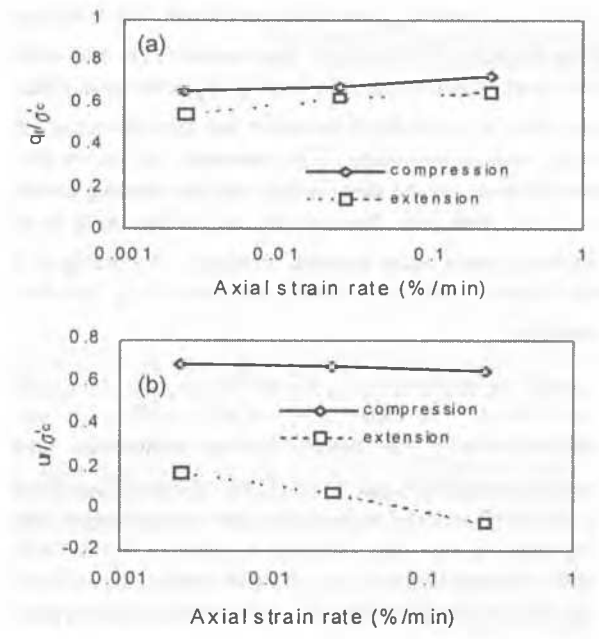

Figs.3(a) and 3(b) show the relationship of the normalized shear strength (q_f/σ'_h) and excess porewater pressure (u_f/σ'_h) at failure versus axial strain rate (log scale) (σ'_c shall be σ'_h)

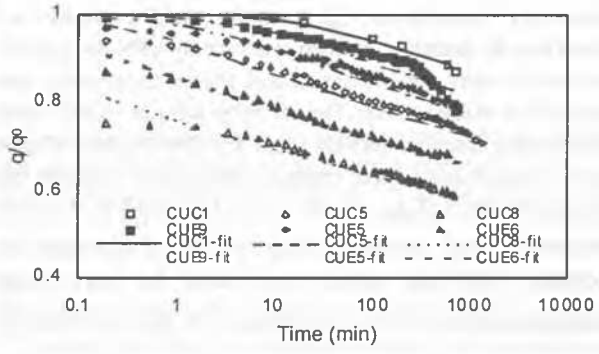

Fig.4 (a) Relationship of q/q_o *vs.* log(time) in stress relaxation of HKMD

Fig.4 shows the relationship of the deviator stress ratio, q/q_0, and the time in logarithmic scale since the start of the stress relaxation. As shown in Fig.4, the relationship of $q/q_0 - \log t$ is almost linear for time period of $t>t_0$ up to the time ending the test. From Fig.4, it is found that lower axial strain rate will result in larger t_0. The slope s is approximately constant for all these tests and appears to be independent of the effective confining pressure. It can also be found that for both compression and extension tests, the slope of s is almost the same. In Fig.4, however, it is obvious that the magnitude of the decay of q/q_0 with time is different for different tests, although the slope s is almost constant. It is evident that the magnitude of the decay of q/q_0 with time is related to the shearing strain rates before the beginning of stress relaxation.

In both compression and extension tests, the porewater pressure increased during relaxation. Under compression states the porewater pressure (Δu) developed in the process of relaxation is small. The ratio of $\Delta u/\sigma'_h$ is about 1.5% - 5.4%. However, the porewater pressure in extension tests is much larger with the ratio of $\Delta u/\sigma'_h$ ranging from 8% to 12.3%.

Although the relationship between q/q_0 and log(t) is nearly linear for a certain time period as shown in Fig.4 and may be expressed approximately by a linear equation after a certain time t_0, the Eqn.(2) has at least two defects. One is that Eqn.(1) is not valid for $t<t_0$. The second is that when t is large enough, q/q_0 in Eqn.(1) may be negative. This is evidently incorrect. Zhu *et. al.* (1999) have suggested a new power law equation, which is free from these defects, to calculate the deviator stress decrease in stress relaxation.

4.3 *Results of Consolidated and Undrained Triaxial Creep Tests*

Two multi-stage undrained triaxial creep tests were performed. Both specimens were normally and isotropically consolidated under the given effective confining pressures. After consolidation a deviator stress in the first stage of creep was applied abruptly and held constant for a period of time for creep to occur. Then the deviator stress was increased again to start the second stage of creep, and so on, until SL=0.99 (SL-Stress Level) in compression states or SL=0.90 in extension states. The multi-stage creep means that one specimen can be used to conduct more than one stage of creep testing.

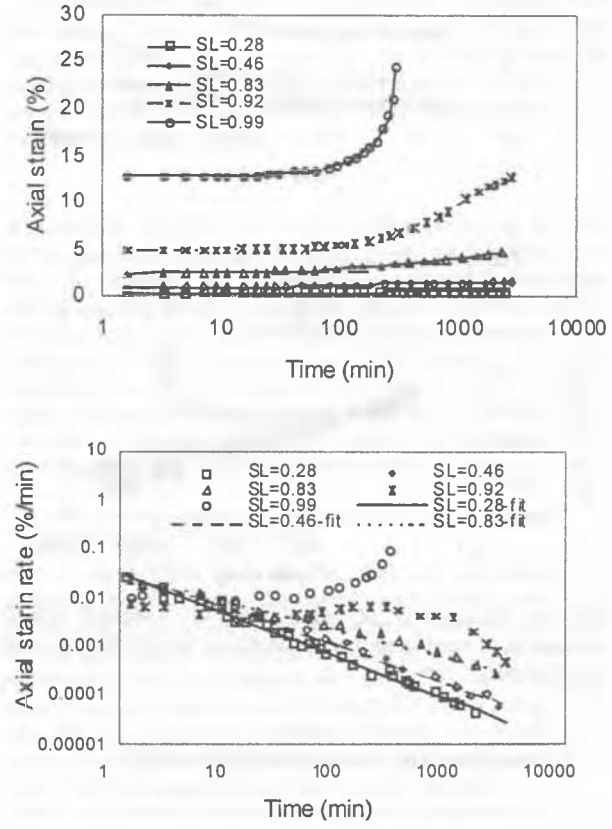

Fig.5 (a) Relationship of axial strain *vs.* log(time) and (b) relationship of axial strain rate *vs.* log(time) in a multi-stage creep test in compression state

For compression creep tests, there were seven stages of creep testing on a single specimen. The development of axial strain with time (log scale) at various levels of deviator stress is shown in Fig.5(a). For clarity, presented in Fig.5(a) are only results of five stages of creep testing. Fig.5(b) presents the variation of axial strain rate of creep with time. It appears that with (stress level) SL $\leq$ 0.83 the relationship of log ($\dot{\varepsilon}_a$) - log t is linear

within the time tested. The line in Fig.5(b) is the fitting line using an equation proposed by Zhu *et. al.* (1999).

There were four stages in the triaxial extension creep test on a single specimen. Fig.6 presents the relationships of axial strain and axial strain rate *vs.* log(time). It can been seen that curves in Fig.6 are similar to those in Fig.6. In the log ($\dot{\varepsilon}_a$) - log t plot, the curves intersect. Within the time observed, the relationship under lower stress levels is linear, and lower stress levels correspond to steeper lines. Comparing Fig.5 with Fig.6, some differences can be found. In the compression creep test, the stress level at which failure occurred is SL=0.99, and the rupture life (time from the initiation of current creep step until final collapse) is about 300 minutes. The rupture life is only a little longer (about 560 minutes) in the extension creep test, while the corresponding stress level is SL=0.90. This implies that specimens under extension states are more susceptible to creep than under compression states. This needs more tests to conform.

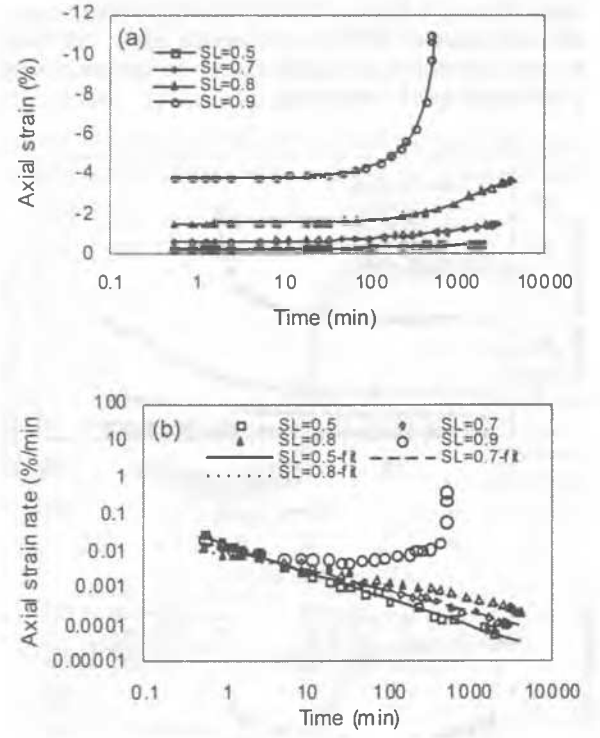

Fig.6 (a) Relationship of axial strain *vs.* log(time) and (b) relationship of axial strain rate *vs.* log(time) in a multi-stage creep test in extension state

5 A NEW ELASTIC VISCO-PLASTIC MODEL

Yin and Graham's (1999) 3-D Elastic Visco-Plastic (3-D EVP) constitutive relationship can be expressed as

$$\dot{\varepsilon}_{ij} = \dot{\varepsilon}_{ij}^{e} + \dot{\varepsilon}_{ij}^{vp} = \left(\frac{1}{2G}\dot{s}_{ij} + \frac{\kappa}{3V}\frac{\dot{p}'}{p'}\delta_{ij} \right) + \frac{\psi}{Vt_0} exp\left[\left(\varepsilon_{vm0}^{r} + \frac{\lambda}{V} ln\frac{p_m'}{p_{m0}'} - \varepsilon_{vm} \right)\frac{V}{\psi} \right] \frac{1}{2p' - p_m'}\frac{\partial F}{\partial \sigma_{ij}'} \quad (4)$$

where $\dot{\varepsilon}_{ij}$ is the total strain rate (i=1,2,3; j=1,2,3); $\dot{\varepsilon}_{ij}^{e}$ and $\dot{\varepsilon}_{ij}^{vp}$ are the elastic and visco-plastic strain rate; σ_{ij}' is effective stress; the mean effective stress p' is defined as $p' = \sigma_{kk}'/3$; $\dot{s}_{ij}$ is the deviator stress rate; the deviator stress s_{ij} is defined as $s_{ij} = \sigma_{ij}' - \delta_{ij}\sigma_{kk}'/3$, where $\delta_{ij} = 0$ if i≠j, $\delta_{ij} = 1$ if i=j; G is elastic shear modulus; κ/V (V is specific volume), ψ/V and t_o, λ/V, p_{mo}' and ε_{vm0}^{r} are model parameters. The F in Eqn.(4) is the function of visco-plastic flow surface (Yin and Graham 1999) is an elliptic surface. In Eqn.(4), p_m' is the mean effective stress value at which the flow surface intercepts the mean effective p' –axis in q-p' plane. The sub-index "m" stands for the mean stress or volume strain under isotropic stressing condition or $p' = p_m'$ with q=0. For example, ε_{vm} in Eqn.(4) is the total volumetric strain under isotropic stressing. According to Yin and Graham (1989, 1994, 1999), the rate of ε_{vm} can be expressed as

$$\dot{\varepsilon}_{vm} = \frac{\kappa}{Vp_m'}\dot{p}_m' + \frac{\psi}{Vt_0} exp\left[\left(\varepsilon_{vm0}^{r} + \frac{\lambda}{V} ln\frac{p_m'}{p_{m0}'} - \varepsilon_{vm} \right)\frac{V}{\psi} \right] \quad (5)$$

The total strain ε_{vm} in Eqn.(4) can be obtained by solving Eqn.(4) numerically. Eqns.(4 and (5) are differential equations of the 3-D EVP model for describing the time-dependent stress-strain behaviour of clays. Readers can refer to Yin & Graham (1999) for more details of the 3-D EVP model, the method for determination of mode parameters and verification of the model.

6 CONCLUSIONS

Good correlations have been established for the compression index C_c, unloading/reloading index C_r, and the coefficient of "secondary" consolidation $C_{\alpha e}$. From the triaxal test results, it is found that the undrained strength increased by 4.9% for a 10-fold increase in strain rate in conventional triaxial compression tests, and 9.3% in extension tests. The porewater pressure increase under compression states is relatively small with the variation of strain rates, but much larger under extension states. Stress relaxation tests showed that ratios of $\Delta u/\sigma_h'$ are 1.7% - 5.4% and 8% - 12.3% for compression and extension tests. In both compression and extension multi-stage triaxial creep tests, the log($\dot{\varepsilon}_a$)-log(t) relationship of lower stress level is linear. The slopes of these lines are dependent on current deviator stress as well as stress history.

REFERENCES

Nakase, A., Kamei, T. and Kusakabe, O. 1988. Constitutive parameters estimated by plasticity index. *J. of Geotechnical Engineering*, ASCE, Vol.114, GT7, pp.844-858.

Graham, J., Crooks, J. H. A., and Bell, A. L., 1983. Time Effects on the Stress-Strain Behavior of Natural Soft Clays. *Geotechnique*, Vol. 33, pp. 327-340.

Yin, J.-H. and Graham, J. 1989. Visco-elastic-plastic modelling of one-dimensional time-dependent behaviour of clays. Canadian Geo-technical Journal, Vol. 26, pp. 199-209.

Yin, J.-H. and Graham, J. 1994. Equivalent times and one-dimensional elastic visco-plastic model-ling of time-dependent stress-strain behaviour of clays. Canadian Geotechnical Journal, Vol. 31,pp. 42-52.

Yin, J.-H. and Graham, J. 1999. Elastic visco-plastic modelling of the time-dependent stress-strain behaviour of soils. Canadian Geotechni-cal Journal, Vol.36, No.4, pp.736-745.

Zhu, J.-G., Yin, J.-H. and Luk, S.T. 1999. Time-dependent stress-strain behaviour of soft Hong Kong marine deposits. Geotechnical Testing Journal, ASTM, Vol.22, No.2, pp.112-120.